A FINITE ELEMENT ANALYSIS ON FATIGUE FAILURE OF A LADDER CHASSIS FRAME DUE TO WELDING RESIDUAL STRESS AND THE TECHNIQUES TO CONTROL IT

Shubhasish Chowdhury[1], Ratan Kumar Das[2*]

[1]Department of Mechanical Engineering, Chittagong University of Engineering and Technology, Chittagong-4349, Bangladesh.
[2]Department of Mechanical Engineering, Chittagong University of Engineering and Technology, Chittagong-4349, Bangladesh.
shubhasishchy.me@gmail.com[1], ratan.kumar@cuet.ac.bd[2*]

Abstract- *In this study fatigue failure caused by welding residual stresses on a ladder chassis frame is discussed with necessary techniques and methods to reduce it. Generally residual stress occurs when the welded joints contradict heat at a different rate than the hot frame surface. It is found that the residual stresses evolved during MIG welding mainly depend on three criterions including welding time, cooling period of the welded joints and the weld bead thickness. A numerical analysis has been carried out in this study to find out the effects of the above three criterions on the residual stress formation during MIG welding and the fatigue failure of the chassis frame. The welded joints in a ladder chassis frame are of T type and the whole study is carried out for different welding and cooling time span with variable weld bead thickness. The results are divided into two parts with one part displays maximum residual stresses against the three criterions separately and the other part discusses fatigue failure of the chassis frame through maximum shear stress and distortion energy failure theory by means of safety factor. The obtained results from the numerical analysis are quite familiar with our expectations as the residual stress changes drastically with the change of these three criterions.*

Keywords: Ram Chassis Frame, Residual Stress, Welding time, Cooling time, Weld bead thickness

1.INTRODUCTION

In a structural steel chassis frame horizontal cross members are connected to the main frames through welded joints between them. During welding process the weld area is heated up sharply relatively to the surrounding area and fused locally. The material expands as a result of being heated. The heat expansion is restrained by the surrounding colder area which gives rise to thermal stresses. In the areas of the component which have cooled down last, tensile stresses occur where thermal stress dominates, and compressive stresses where transformation stress dominates [1]. Researchers have carried out numerical studies on the failure of the chassis frame, but a major chunk of this studies are concerned about the failure due to buckling, vibrations and torsional stiffness. A few researches have been carried out on welding residual stress failure. Among them Rahul Shivaji et al. found that the yielding of the chassis frame decreases with the gradual decrease of the weld throat size and the frame can sustain more load [2]. C. Hackmair et al. did investigations which focus on the simulation of the welding sequence and its effect on distortions for the front axle carrier of the new BMW series 7 [3]. The studies mentioned above failed to describe the fatigue failure criterion of the chassis frame, no specific details have been given on which geometrical part of the chassis frame would yield first whether the horizontal crossbars or the mainframe, and no specific factors have been discussed which influences the residual stress formation rate. In this study a finite element analysis of the T-welded joints of a chassis frame has been carried out to show the fatigue failure of the bars and the frame due to thermal residual stresses with necessary factors being discussed which are believed to be the controllers of the thermal residual stress formation during welding.

Many researchers have described welding residual stress phenomenon through numerical analysis and identified various reasons which affects the rate of residual stress formation. Among them H. Long et al. carried out numerical analysis of the butt joints of thin plates to predict welding distortion. It is found that higher longitudinal shrinkages occur in the weld than in the outer rim of the plate and the largest transverse shrinkage occurs at the middle section of the length of the plate and it gradually reduces towards to the starting and ending edges of the welding line [4]. D. Gery et al. found that the increase of the welding speed causes temperature decrease mainly in fusion zone but has a less effect to the areas outside of fusion zone and heat affected zone for butt welded joints. As a result residual stresses would be predominant at the high temperature zone [5]. X. K Zhu et al. performed numerical simulation of friction stir welding of 304L stainless steel and found that the residual stress in the welds after fixture release decreases as compared to those before fixture release [6].

Peng-Hsiang Chang et al. performed numerical analysis of butt-welded joints and found that a very large tensile longitudinal residual stress and a high transverse residual tensile stress occur near the weld toe, and a compressive stress appears away from the weld bead [7]. Dean Deng found that the phase transformation has no effect on the welding residual stress for low carbon steel but has an significant effect in the case of medium carbon steel [8]. He also carried out numerical simulation of temperature field and residual stress in multi-pass welds in stainless steel pipe and found that the temperature distribution around the heat source is uniform and in weld zone and its vicinity, a tensile axial residual stress is produced on the inside surface, and compressive axial stress at outside surface [11]. Y. C. Lin et al. introduced preheating during weldment of 304 stainless steel and found that the welding residual stress not being improved significantly with preheating with the residual stress increases with the increase of preheat temperature [9]. M. Peel et al. investigated the dependence of microstructure, mechanical properties and residual stresses on the welding speed during aluminum friction stir welding. It was found that the weld properties are dominated by the thermal input rather than the mechanical deformation by the tool [12]. Tso-Liang Teng et al. investigated the effect of welding conditions on residual stresses due to butt welds and found that the middle weld bead is in tension and the magnitude of this stress equals the yield stress [13]. B. Taljat et al. carried out numerical analysis of GTA welding process to investigate the phase transformation effects on the residual stresses and found that the volumetric changes associated with the austenite to martensite phase transformation in HY-100 steel significantly affect residual stresses in the weld fusion zone and the heat affected zone [14]. From the analysis of above studies three criterions are selected for the present study to analyze the effect of them on welding residual stress. The criterions are welding time, cooling period of the welded joints and the weld bead thickness. A comparative analysis has been carried out in this study for variable welding and cooling time along with variable weld bead thickness to have a clear view of their effects on fatigue failure of the chassis frame.

2. METHODOLOGY

The whole numerical analysis is carried out in ANSYS 16.0 and the CAD model is designed in SOLIDWORKS 2012.

2.1 Research Model

Fig.2.1: CAD drawing of the proposed chassis model

A suitable chassis frame model was drawn in SOLIDWORKS 2012 and shown below is a simple replica of a DODGE RAM pickup chassis.

2.2 Model Description

The CAD model has many horizontal bars of different shapes which are welded to the main two HSS frame. For the better analysis a simple model is needed which is taken from the rear end of the chassis frame by sectioning it which is shown below in the figure 2.3. The model has two bars welded to the main HSS frame.

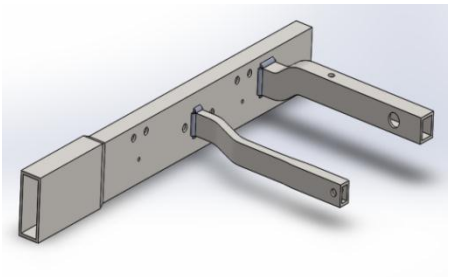

Fig.2.2: Ram model part (after sectioning)

2.3 Chassis Frame Material

In this study, structural steel is used as a frame material. The structural steel or carbon steel has 2.1% carbon and the welding temperature for the carbon steel is 1130^0C.

2.4 Heat Transfer Medium

The heat transfer or loss from the hot frame surface takes place through convection and radiation. In this study convection medium is assumed as stagnant air and a tabular data is defined for convection coefficient of stagnant air which is variable with the change of frame surface temperature. The tabular data is taken from ANSYS convection data samples for stagnant air-vertical plane1. The emissivity of the surrounding is assumed 0.8.

2.5 Governing Equations

Conduction Heat Transfer:

$$q_x = -kA(\partial T/\partial x)$$

$$\frac{\partial^2 T}{\partial x^2} + \frac{\partial^2 T}{\partial y^2} + \frac{\partial^2 T}{\partial z^2} + q.\frac{1}{k} = \partial T/\ \alpha\ \partial\tau \qquad \text{Eq. (1)}$$

Where the quantity α = k/ρc is called the thermal diffusivity of the material [10].

Transient Heat Transfer Numerical Method [10]

X-Y plane:

$$k\left(\frac{\partial^2 T}{\partial x^2} + \frac{\partial^2 T}{\partial y^2}\right) = \rho c\left(\frac{\partial T}{\partial \tau}\right) \qquad \text{Eq. (2)}$$

$$\frac{\partial^2 T}{\partial x^2} = (T_{m+1,\,n} + T_{m-1,\,n} - 2T_{m,\,n}) / (\Delta x)^2$$

$$\frac{\partial^2 T}{\partial y^2} = (T_{m,n+1} + T_{m,n-1} - 2T_{m,\,n}) / (\Delta y)^2$$

Y-Z plane:

$$k\left(\frac{\partial^2 T}{\partial y^2} + \frac{\partial^2 T}{\partial z^2}\right) = \rho c\left(\frac{\partial T}{\partial \tau}\right) \qquad \text{Eq. (3)}$$

$\frac{\partial^2 T}{\partial y^2} = (T_{n+1,\,p} + T_{n-1,\,p} - 2T_{n,\,p}) / (\Delta y)^2$

$\frac{\partial^2 T}{\partial z^2} = (T_{n,\,p+1} + T_{n,\,p-1} - 2T_{n,\,p}) / (\Delta z)^2$

Z-X plane:

$$k\left(\frac{\partial^2 T}{\partial z^2} + \frac{\partial^2 T}{\partial x^2}\right) = \rho c\left(\frac{\partial T}{\partial \tau}\right) \quad \text{Eq. (4)}$$

$\frac{\partial^2 T}{\partial z^2} = (T_{p+1,\,m} + T_{p-1,\,m} - 2T_{p,\,m}) / (\Delta z)^2$

$\frac{\partial^2 T}{\partial x^2} = (T_{p,m+1} + T_{p,\,m-1} - 2T_{p,m}) / (\Delta x)^2$

The subscript m denotes the x position; the subscript n denotes the y position and the subscript p denotes the z position.

Maximum Equivalent Stress Safety tool (ANSYS Workbench): The theory states that a particular combination of principal stresses causes failure if the maximum equivalent stress in a structure equals or exceeds a specific stress limit.

$\sigma_e \geq S_{limit}$

Expressing the theory as a design goal:

$\sigma_e / S_{limit} < 1$

$\sigma_e / S_y < 1$

$\sigma_e / S_u < 1$

Safety Factor: $F_S = S_{limit} / \sigma_e$ Eq. (5)

Maximum Shear Stress Safety tool (ANSYS Workbench): The theory states that a particular combination of principal stresses causes failure if the Maximum Shear equals or exceeds a specific shear limit:

$\tau_{max} \geq f\, S_{limit}$

Expressing the theory as a design goal:

$\tau_{max} / f\, S_{limit} < 1$

$\tau_{max} / f\, S_y < 1$

$\tau_{max} / f\, S_u < 1$

Safety Factor: $F_S = fS_{limit} / \tau_{max}$ Eq. (6)

Fatigue Safety Tool [15]: The analysis is based on mean stress life of the chassis frame with the criteria of failure used in the analysis is soderberg. The criterion equation for the Soderberg line is:

$$(\sigma_a / S_e + \sigma_m / S_y) = 1 / n \quad \text{Eq. (7)}$$

3. CASE STUDIES and CONDITIONS

The effect of three case studies on the residual stress formation would be discussed. They are:

1. Effect of welding time on residual stresses.
2. Effect of cooling period on residual stresses.
3. Effect of weld bead thickness on residual stresses.

3.1 Boundary Conditions

The heat loss from the hot boundary surface is encouraged by convection heat transfer through the stagnant air film. The heat loss is defined by the equation:

$$q/A = h\,(t_S - t_f) \quad \text{Eq. (8)}$$

Where q/A is heat flux out of the face, h is the film coefficient, t_s is the temperature on the face and t_f is the bulk fluid temperature [10]. The heat loss through radiation can be described by the equation:

$$q_{emitted} = \sigma A T^4 \quad \text{Eq. (9)}$$

Where, σ is called the Stefan-Boltzmann constant with the value of 5.669×10^{-8} W/m^2 · K^4 [10].

The thermal residual stress occurring on the frame surface can be defined through the following equation:

$$\sigma_e = F/A = Y\alpha\Delta T \quad \text{Eq. (10)}$$

Where Y is Young's Modulus of the material, α is the coefficient of linear thermal expansion, and ΔT is the change in temperature.

3.2 Initial Conditions

1. The two HSS horizontal bars are assumed to be welded at the same time with no preheating is done.
2. The analysis model is fixed with zero degree of freedom.
3. Heat contradiction rate of the weld beads is faster means the welded joints will cool first.

3.3 Conditions Used in Case Studies

Effect of Welding Time: Only welding time is variable. Cooling period and weld bead thickness is fixed. Welding time is taken for 1 to 5 minutes. Cooling period of the welded joints is assumed 9 minutes with weld bead thickness is 4 mm.

Effect of Cooling Time: Only cooling time is variable. Welding time and weld bead thickness is fixed. Cooling period is taken for 10 to 50 minutes. Welding time of the welded joints is assumed 2 minutes with weld bead thickness is 4 mm.

Effect of Weld Bead Thickness: Welding time and cooling time are assumed constant. Weld bead thickness varies from 1 to 5 mm. Welding time of the welded joints is assumed 3 minutes with cooling period assumed 9 minutes.

4. RESULTS AND DISCUSSION

The heat evolves during welding is maximum at the welded joints which is the heat source here, so the temperature at that region is also maximum. With the increase of distance from the heat source, the temperature distribution during welding slows down and we can see from the figure 4.1 that the temperature on the rest of the frame (except regions closer to welded joints) is close to ambient temperature marked by the blue color region.

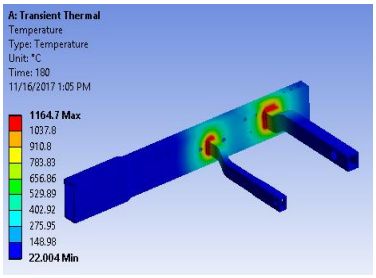

Fig.4.1: Temperature distribution during welding

Figure 4.2 shows the temperature distribution on the chassis frame after the hot welded joints have been cooled down by external means. It is found that the temperature

distribution is still maximum on the main HSS frame comparing to the other two HSS horizontal bars after the weld beads have been cooled down to the ambient temperature.

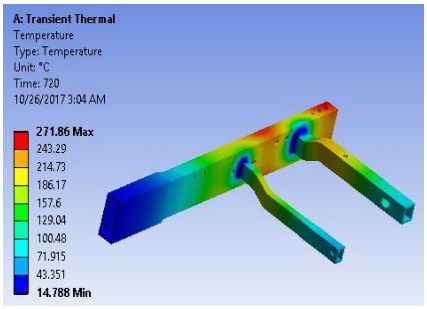

Fig.4.2: Temperature distribution after cooling

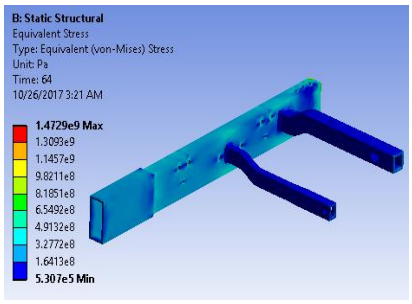

Fig.4.3: Equivalent stress on the chassis frame

Figure 4.3 and figure 4.4 show the corresponding equivalent stress and shear stress distribution on the chassis frame. Without referring to any of the three case studies the results show that the stresses are maximum on HSS frame and minimum occurs on the two bars.

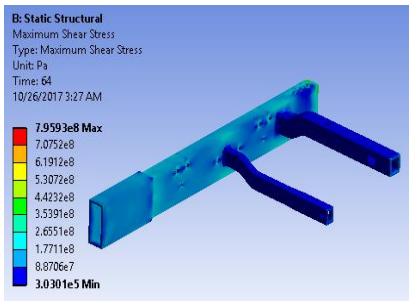

Fig.4.4: Maximum shear stress on the chassis frame

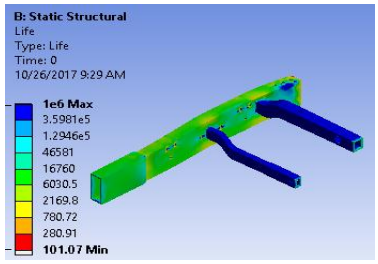

Fig.4.5: Fatigue life analysis of the chassis frame

Figure 4.5 shows the available life of the chassis frame after the welded joints have been cooled to the ambient temperature. It shows that the bars would last more than the main frame as the available life of the bars is maximum 10^6 cycles. Figure 4.6 shows the safety factor guarding against the fatigue failure due to yielding. It is found that the main frame is prone to fatigue failure due to yielding which is marked by the critical red color.

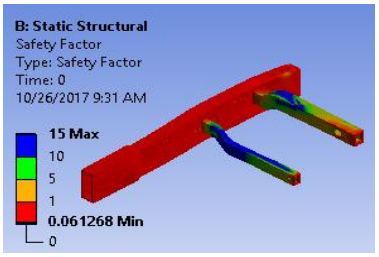

Fig.4.6: Safety factor guarding fatigue failure

The results obtained from the analysis of three case studies are discussed below:

4.1 Effect of Welding Speed or Time

Figure 4.7 and figure 4.8 shows that the residual equivalent stress and shear stress increase with the increase of welding time.

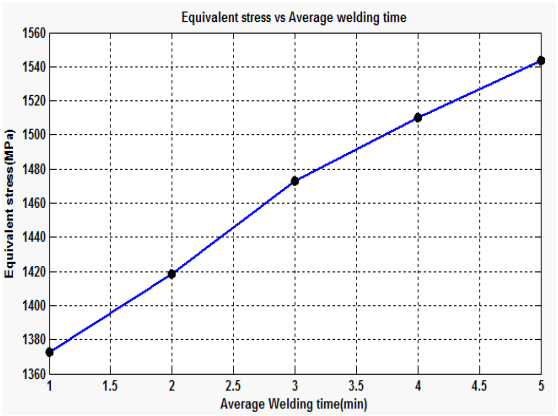

Fig.4.7: Effect of welding time on equivalent stress

When the welding speed increases, the heat addition to the frame and bars also increases as the joining interface region of the bars and the frame is subjected to the high temperature welding flame for additional time.

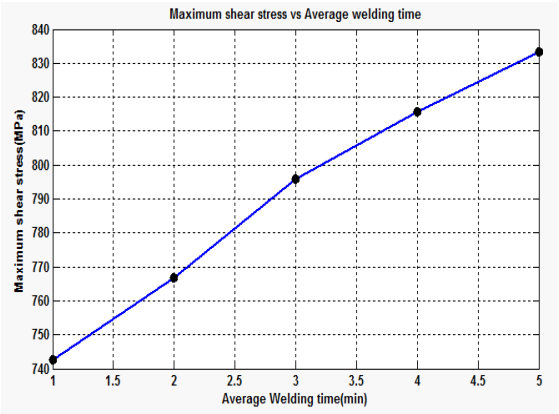

Fig.4.8: Effect of welding time on maximum shear stress

From table 4.1 it is found that the minimum safety factor is below unity for all safety tool analysis. The minimum safety factor is found at the base HSS main frame indicating that the base metal frame would completely fail for the corresponding welding times. The results indicate that the

minimum safety factor guarding maximum equivalent stress and maximum shear stress failure increases with the decrease of welding time. Again from fatigue failure analysis, it is found that the minimum fatigue life and minimum safety factor guarding yielding also increases with the decrease of welding time.

Table 4.1: Safety tool analysis for variable welding time

Welding time (minutes)	Max. equiv. stress failure (min.)	Max. shear stress failure (min.)	Fatigue failure (min.)	
	Safety Factor	Safety Factor	Life (cycles)	Safety Factor
1	0.1821	0.16834	107.41	0.06278
2	0.1762	016299	99.068	0.06076
3	0.1697	0.15705	90.676	0.58524
4	0.1655	015323	85.481	0.05707
5	0.1619	0.14999	81.19	0.05584

*Maximum safety factor= 15 and Maximum fatigue failure life= 10^6 cycles which are observed at the two horizontal HSS bars.

4.2 Effect of Cooling Time

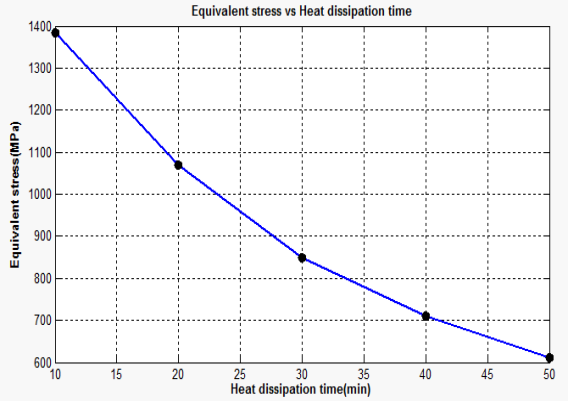

Fig.4.9: Effect of cooling time on equivalent stress

Figure 4.9 shows that the maximum equivalent stress decreases with the increase of the cooling time. The results reveal that if the welded joints or weld beads are allowed to cool for a longer time, the residual stresses will drastically decrease as the heat contradiction rate in that case will be low which in turn will produce low compressive stresses.

From table 4.2 it is found that the minimum safety factor is below unity for all safety tool analysis. The minimum safety factor is found at the base HSS main frame and the maximum safety factor is observed at the two HSS bars indicating that the main frame will fail due to yielding. The minimum safety factor guarding maximum equivalent stress and maximum shear stress failure increases with the increase of cooling time. Again from fatigue failure analysis, it is found that the minimum fatigue life and minimum safety factor guarding yielding also increases with the increase of cooling time.

Table 4.2: Safety tool analysis for variable cooling time

Cool. time (minutes)	Max. equiv. stress failure (min.)	Max. shear stress failure (min.)	Fatigue failure (min.)	
	Safety Factor	Safety Factor	Life (cycles)	Safety Factor
10	0.1805	0.16706	105.16	0.06225
20	0.2335	0.21737	199.33	0.08052
30	0.2943	0.27527	363.84	0.1015
40	0.3521	0.3313	579.81	0.12142
50	0.4084	0.3752	852.55	0.14082

*Maximum safety factor= 15 and Maximum fatigue failure life= 10^6 cycles which are observed at the two horizontal HSS bars.

3.3 Effect of Weld Bead Thickness

Figure 4.10 shows that the maximum shear stress increases with the increase of the weld bead thickness. For welding with thicker weld bead needs more welding time and filler metal which in turn increase residual stresses. Moreover thicker weld pool takes time to cool down and the corresponding heat contradiction rate is higher.

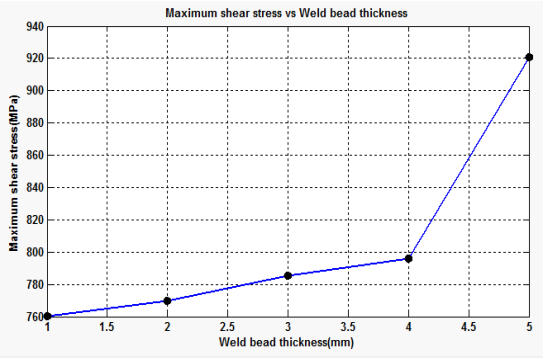

Fig.4.10: Effect of weld bead thick. on max. shear stress

From table 4.3 it is found that the minimum safety factor is below unity for all safety tool analysis. The minimum safety factor is found at the base HSS main frame and the maximum safety factor is observed at the two HSS bars indicating that the main frame will fail due to yielding.

Table 4.3 Safety tool analysis for variable weld bead thick.

Weld bead thick. (mm)	Max. equiv. stress failure (min.)	Max. shear stress failure (min.)	Fatigue failure (min.)	
	Safety Factor	Safety Factor	Life (cycles)	Safety Factor
1	0.17769	0.16442	101.07	0.06126
2	0.17548	0.16237	98.081	0.06050

3	0.17195	0.15912	93.492	0.05928
4	0.16973	0.15705	90.676	0.05852
5	0.14828	0.13576	65.941	0.05112

*Maximum safety factor= 15 and Maximum fatigue failure life= 10^6 cycles which are observed at the two horizontal HSS bars.

The minimum safety factor guarding maximum equivalent stress and maximum shear stress failure increases with the decrease of weld bead thickness. Again from fatigue failure analysis, it is found that the minimum fatigue life and minimum safety factor guarding yielding also increases with the decrease of weld bead thickness.

5. CONCLUSION

Emphasis has been given in this study to control thermal residual stress by controlling the above three criterions by considering all the geometrical aspects. The major findings of this numerical study are concluded below:

i. The two bars should be welded one after one not in the same time as the excessive heat evolved during welding is fully damaging the main base metal frame as found in the safety tool analysis.
ii. Faster welding speed or lesser welding time can produce comparatively less residual stress without considering the effect of cooling period of the welded joints and the weld bead thickness.
iii. With the increase of the cooling period the stresses tend to decrease which proves that the lesser heat contradiction rate from the welded joints will form lower residual stresses.
iv. The thickness of arc or weld bead also influences the formation of residual stresses with the arc exceeding the metal frame thickness producing huge residual stresses. Smaller weld bead is favorable due to its low stress formation.

6. ACKNOWLEDGEMENT

This work was partially supported and funded by the department of Mechanical Engineering of Chittagong University of Engineering & Technology as undergraduate project for final year student.

7. REFERENCES

[1] Dieter Radaj, Heat effects of welding: temperature field, residual stress, distortion, 1st edition, pp. 8-15, springer-verlag, Berlin Heidelberg, 1992.
[2] Mr. Yadav (khot) Rahul Shivaji, Mr. Pankaj Bhakare "FEA Based Validation of Weld Joint Used In Chassis of Light Commercial Vehicles (LCV) In Tensile and Shear Conditions" Ijiert, Volume 2, Issue 3 March2015.
[3] C. Hackmair, E. Werner and M. Ponisch "Application of welding simulation for chassis components within the development of manufacturing methods" Computational Materials Science 28 (2003) 540–547.
[4] H.Long, D.Gery, A.Carlier, P.G. Maropoulos "Prediction of welding distortion in butt joint of thin plates" Materials and Design 30 (2009) 4126–4135.
[5] D. Gery, H. Long, P. Maropoulos "Effects of welding speed, energy input and heat source distribution on temperature variations in butt joint welding" Journal of Materials Processing Technology 167 (2005) 393–401.
[6] X.K. Zhu, Y.J. Chao "Numerical simulation of transient temperature and residual stresses in friction stir welding of 304L stainless steel" Journal of Materials Processing Technology 146 (2004) 263–272.
[7] Peng-Hsiang Chang, Tso-Liang Teng "Numerical and experimental investigations on the residual stresses of the butt-welded joints" Computational Materials Science 29 (2004) 511–522.
[8] Dean Deng "FEM prediction of welding residual stress and distortion in carbon steel considering phase transformation effects" Materials and Design 30 (2009) 359–366.
[9] Y. C. Lin and K. H. Lee "Effect of preheating on the residual stress in type 304 stainless steel weldment" Journal of Materials Processing Teclmology 63 (1997) 797-801.
[10] J.P. Holman, Heat Transfer, 10th edition, pp. 1-12 and 147-170, McGraw-Hill Education, New York, 2010.
[11] Dean Deng, Hidekazu Murakawa "Numerical simulation of temperature field and residual stress in multi-pass welds in stainless steel pipe and comparison with experimental measurements" Computational Materials Science 37 (2006) 269–277.
[12] M. Peel , A. Steuwer, M. Preuss, P.J. Withers "Microstructure, mechanical properties and residual stresses as a function of welding speed in aluminium AA5083 friction stir welds" Acta Materialia 51 (2003) 4791–4801.
[13] Tso-Liang Teng, Chih-Cheng Lin "Effect of welding conditions on residual stresses due to butt welds" International Journal of Pressure Vessels and Piping 75 (1998) 857–864.
[14] B. Taljat, B. Radhakrishnan, T. Zacharia "Numerical analysis of GTA welding process with emphasis on post-solidification phase transformation effects on residual stresses" Materials Science and Engineering A246 (1998) 45–54.
[15] Richard G. Budyans and J. Keith Nisbett, Shigley's Mechanical Engineering Design, 10th edition, pp. 274-308, McGraw-Hill Education, New York, 2015.